Melting of model structures: molecular dynamics and Voronoï tessellation

1997 J. Phys.: Condens. Matter 9 4051

(http://iopscience.iop.org/0953-8984/9/20/005)

J. Phys.: Condens. Matter **9** (1997) 4051–4059. Printed in the UK PII: S0953-8984(97)80230-5

Melting of model structures: molecular dynamics and Voronoï tessellation

P Jund†, D Caprion†, J F Sadoc‡ and R Jullien†

† Laboratoire des Verres, Université Montpellier 2, Place E Bataillon, Case 069, 34095 Montpellier, France

‡ Laboratoire de Physique des Solides, Université Paris-Sud, 91405 Orsay, France

Received 10 December 1996

Abstract. Using classical molecular dynamics simulations combined with Voronoï tessellation we study the geometrical modifications as a function of temperature in two model Frank–Kasper phases: the A15 structure (β-tungsten) and the cubic Friauf–Laves structure ($MgCu_2$). We show how the perfect arrangement of disclination lines at 0 K for the crystalline structures evolves through the melting point. In particular, as the temperature is increased, the results permit us to identify the first defect and to show that the initial network of disclination lines survives until the solid–liquid first-order transition has indeed taken place.

1. Introduction

In the past ten years compact tetrahedral phases, called Frank–Kasper phases [1], have received renewed attention because of their connection with quasicrystalline phases [2] and also because new phases have been discovered recently [3]. As regards the geometrical approach, these phases have an additional advantage since they appear as a solution to frustration [4].

In this study we want to focus on the simplest of these phases, namely the structure of β-tungsten, also called A15, and the cubic Friauf–Laves structure of $MgCu_2$. These structures are not only the simplest, but also correspond to the lowest and the highest coordination numbers in Frank–Kasper structures [4]. These structures are well described using the major skeleton formed by the Frank–Kasper lines, which are the lines joining atoms without an icosahedral local order. The A15 structure is an example in which these lines never intersect, whereas the Friauf–Laves structure is an example in which all Frank–Kasper lines intersect at the atomic sites. This high degree of icosahedral order is reflected best in the geometrical characteristics of the Voronoï cells, which are the extensions of the Wigner–Seitz cells defined for periodic lattice nodes. On the other hand, the evolution of these lines with temperature has not been investigated or modelled, even though it seems that a description of this evolution would provide the most efficient way to characterize how the icosahedral order is affected by temperature, or, in other words, how these Frank–Kasper phases melt. Therefore, we combined molecular dynamics simulations and the Delaunay–Voronoï tessellation to follow dynamically the evolution of the geometrical characteristics of the Voronoï cells as a function of temperature, in order to shed new light on the melting of Frank–Kasper phases from a *geometrical* point of view.

In section 2 a description of the method and the model structures will be given. We present and discuss our results in section 3. Finally in section 4 we present our conclusions.

0953-8984/97/204051+09$19.50

2. The method and model systems

2.1. The method

We performed molecular dynamics simulations for microcanonical systems of soft spheres interacting via the inverse-sixth-power potential defined by Laird and Schober [5]:

$$U(r) = \epsilon\left(\frac{\sigma}{r}\right)^6 + Ar^4 + B. \tag{1}$$

To simplify the simulations, the potential was cut off at $r/\sigma = 3.0$, and A and B were chosen such that the potential and the force are zero at the cut-off.

Our simulations used a rigid cubic box of edge length L, with periodic boundary conditions (PBC) at constant density. To integrate the equations of motion we use the fourth-order Runge–Kutta algorithm.

This potential has been chosen by analogy with previous work on glasses [6]. It is an efficient potential, when applied to constant-volume simulation, in order to lead to glasses after quenching the liquid. Clearly, it is not at all our purpose to simulate true metallic Frank–Kasper phases, which would need a more sophisticated potential to be in the thermodynamic ground state. Note here that Frank–Kasper phases are not only encountered in metallic alloys, but also appear as micellar ordered structures for amphiphilic molecules in water solutions. They are also related to clathrate structures.

Starting from initial samples at 0 K, the following configurations were obtained by annealing the samples at an annealing rate of 10^{12} K s^{-1}, which was achieved by adding the corresponding amount of energy to the total energy of the system at each iteration.

At several temperatures during this annealing process, the configurations (positions and velocities) were saved. Each configuration was then used to start a constant-energy molecular dynamics calculation during which the temperature was recorded as a function of time. In all cases, we observed a relaxation process typical of such a system [7] during which a slight increase of the temperature was observed before a saturation regime was instigated. We found that typically 10 000 iterations were enough to ensure that we obtained a well defined constant temperature for each sample. After these 10 000 relaxation steps, we started to calculate the geometrical quantities, which were then monitored during 20 000 additional steps.

In fact, during these additional steps we combined our molecular dynamics scheme and the so-called 'Voronoï–Delaunay tessellation', which was originally introduced to analyse random close packings of spheres [8–10]. The Voronoï cell is defined as the ensemble of points closer to a given atom than to any other, and it is characteristic of the local environment around the given atom. To obtain it we have used an efficient algorithm which has been recently introduced to study large random sphere packings [11]. The first step of this algorithm is to determine the Delaunay tetrahedral simplicial cells for a given configuration. These cells are—among all of the tetrahedra formed with four atomic centres—the ones such that no other atomic centre lies inside their circumscribed spheres. This part is the most computer time demanding, but our algorithm (which takes care of the PBC) is efficient enough to be included within the molecular dynamics code. As an input, one has to provide a cut-off distance which should be larger than the longest edge of all of the simplicial tetrahedra. If this is not case, the basic requirement—namely that the sum of the volumes of all of the simplicial tetrahedra is equal to the volume of the simulation box—is not fulfilled, and the algorithm has to be run again with a new and larger cut-off. Once the simplicial tetrahedra are obtained, the Voronoï cell of a given atom is determined, in the knowledge that its vertices are the centres of the circumspherical spheres of all of the

simplicial tetrahedra sharing this atom. During the simulation, we recorded the geometrical characteristics of these cells; among these were the mean number of faces $\langle F \rangle$, also called the coordination number z, as well as the fractions f_e of cell faces having a given number e of edges ($e \geqslant 3$).

2.2. Model systems

2.2.1. A15 structure (β-tungsten). The unit cell of this structure is a cube (length = 1.0) containing eight atoms. This cube contains a centred icosahedron, with the twelve external atoms located on the faces of the cube. The vertices of the cube are also occupied. Among the eight atoms in the primitive cell, two of them have an icosahedral coordination shell ($z = 12$) while the others in the cell faces have $z = 14$. They are usually called Z_{12} and Z_{14}. Connecting the non-icosahedral Z_{14} sites, a triple periodic array of infinite non-intersecting Frank–Kasper lines threads 'hexagonal' faces (see figure 2(a)). Therefore, at 0 K, the perfect structure has an average coordination number $\langle z \rangle = 13.5$, while $f_5 = 0.89$ and $f_6 = 0.11$.

For this structure, simulations were done with 1000 particles, using $\sigma = 0.5$ and $\epsilon/k_B = 100$ K. The length of the simulation box was taken equal to $L = 5.0$, and the mass of the particles was fixed to 50 amu. For the simulation, 5.0 fs was found to be an adequate time step.

2.2.2. Cubic Friauf–Laves structure ($MgCu_2$). The cubic unit cell (length = 1.0) contains eight atoms of Mg type with a distance $d_{\mathrm{Mg-Mg}} = 0.43$ in a diamond-like structure, and sixteen atoms of Cu type with a distance $d_{\mathrm{Cu-Cu}} = 0.35$ located in the tetrahedral interstices of the diamond structure. For the latter the coordination shell is a slightly deformed icosahedron ($z = 12$), while for the former, it contains 16 vertices ($z = 16$). They are usually called Z_{16}. The non-icosahedral Z_{16} sites can be connected by lines leading to a Frank–Kasper major skeleton. But in this case there are four segments meeting at a site, so they form a network similar to that formed by bonds in a diamond structure. Therefore, at 0 K, the perfect structure has an average coordination number $\langle z \rangle = 13.33$, while $f_5 = 0.9$ and $f_6 = 0.1$.

For this structure, simulations were done with 648 particles, using $\sigma_{\mathrm{Cu}} = 0.28$ and $\sigma_{\mathrm{Mg}} = 0.34$. The length of the simulation box was taken equal to $L = 3.0$, and the time step was adjusted to 2 fs.

2.3. Frank–Kasper lines as disclinations

It is an attractive method to consider Frank–Kasper structures as crystals of defects [12]. Introducing defects must be done by reference to a perfect order, which in this case is the icosahedral order: in a Frank–Kasper structure all places where the local order is not icosahedral are defects. The Frank–Kasper lines connect these defects. On the other hand, a perfect icosahedral order can exist only in a positively curved space [13]; therefore the defects needed to balance the curvature should introduce a concentration of negative curvature, which is a property of disclinations. In fact, using this terminology, Frank–Kasper lines are disclination lines appearing on bonds shared by six tetrahedra instead of five for the perfect icosahedral order. By definition, Frank–Kasper structures contain only this kind of disclination, but other structures can contain other types of disclination—for example, when a tetrahedron edge is common to four or three tetrahedra. Upon heating we will encounter such defects.

The geometry and the topology of disclinations lines are governed by conservation rules. In fact these lines behave as if they have a line tension proportional to their angular deficit $\delta_e = 2\pi - e\alpha_t$, where e is the number of tetrahedra sharing an edge, and $\alpha_t = \cos^{-1}(1/3)$ is the tetrahedron dihedral angle.

Frank–Kasper lines are a nice example of this behaviour. In the A15 structure, all lines, which never intersect, are straight lines. In Friauf–Laves phases, four segments ending on a node have a highly symmetric configuration. When positive and negative disclinations are mixed, they have to respect such rules; some examples are described below for disclination lines appearing upon heating. It is worth mentioning that in the geometrical approach, a non-pentagonal face of the Voronoï–Delaunay decomposition corresponds to a 'defect', and the corresponding face encircles then a segment of 'disclination line'.

There is also a balance for the space curvature. In order to consider this problem it is helpful to suppose that the structure is not lying in a flat space but in a corrugated one, flat only on average. Curvature concentrations are then located on tetrahedron edges, and they are positive for edges shared by three, four, or five tetrahedra, and negative for edges shared by six or more. In three dimensions there is no exact relation between the f_es resulting from the global vanishing curvature. Nevertheless there exists an approximate relation $\sum_e \delta_e f_e \simeq 0$ [14]. This gives, if we consider that there are only pentagonal and hexagonal faces for Voronoï cells, $f_5 = 0.8958$ and $f_6 = 0.1041$. In the Frank–Kasper structures studied here, f_5 and f_6 are close to these values.

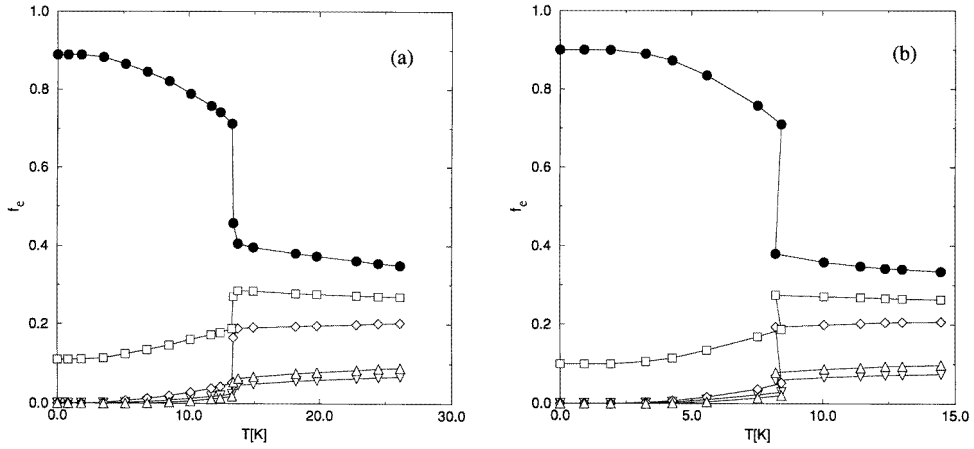

Figure 1. (a) The temperature evolution of the f_es for β-W: $\triangledown$: $e = 3$; $\diamond$: $e = 4$; $\bullet$: $e = 5$; $\square$: $e = 6$; $\triangle$: $e = 7$. (b) As (a), but for $MgCu_2$

3. Results and discussion

3.1. Results

The aim of our study is to follow during the heating process the evolution of the local structure. Therefore we report in figure 1 the variation of the f_es as a function of temperature (once the system has reached equilibrium) for the β-W structure (figure 1(a)) and the $MgCu_2$ structure (figure 1(b)). As expected for a solid–liquid transition, at the transition point the physical parameters are discontinuous, which is typical of a first-order transition. In

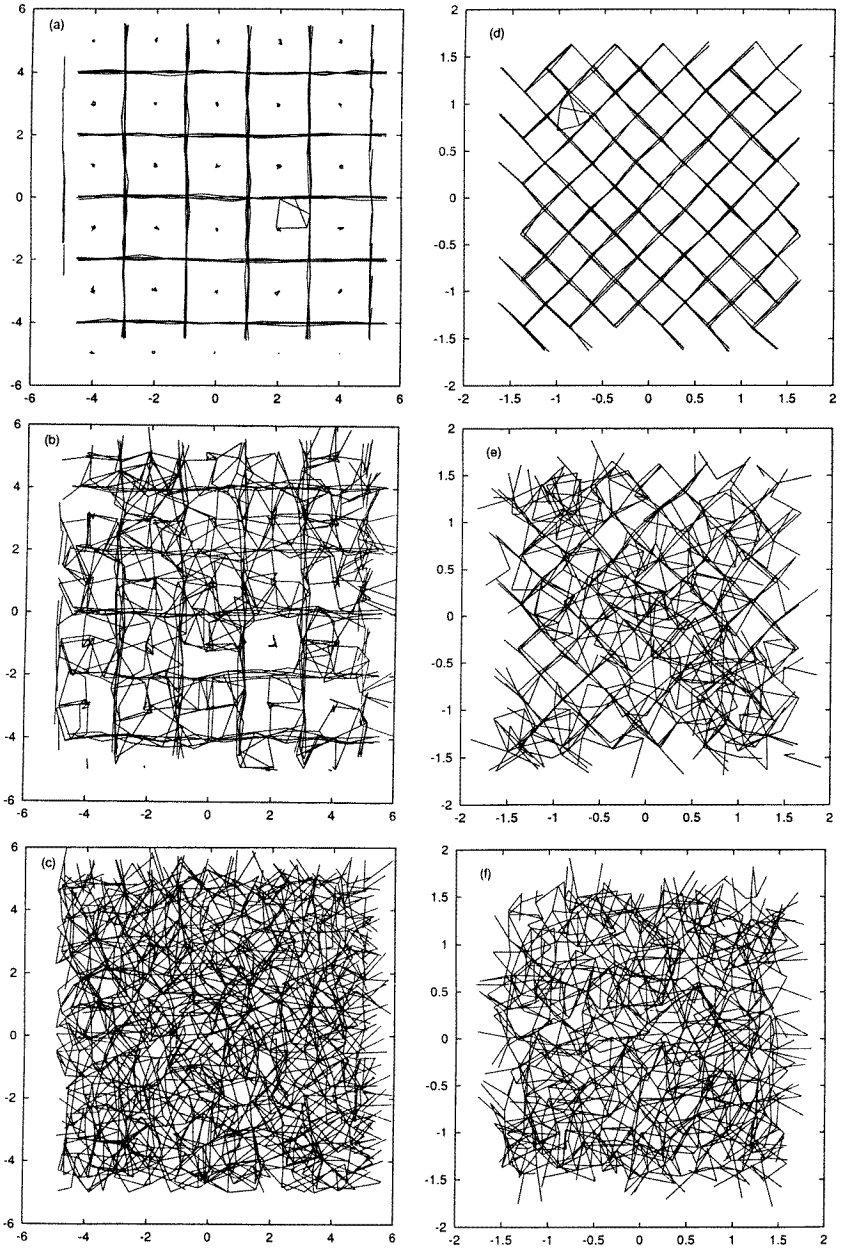

Figure 2. Disclination lines for β-W: (a) $T = 3.5$ K, (b) $T = 13.4$ K, (c) $T = 13.7$ K; and disclination lines for $MgCu_2$: (d) $T = 1.9$ K, (e) $T = 8.5$ K, (f) $T = 8.1$ K.

particular a sharp drop in f_5 can be observed at $T_m \approx 13.5$ K (β-W) and $T_m \approx 8.0$ K ($MgCu_2$), indicating the passage from solid to liquid behaviour. It is worth mentioning that these curves are basically unchanged when for example a faster annealing rate is used (10^{13} K s^{-1}). This indicates that these curves are indeed equilibrium curves. The breakdown of f_5 towards the liquid value of about 0.4 (and the corresponding increase of all of the

other f_es) happens for both structures when $f_5 \approx 0.7$, which indicates that the breaking mechanisms of the icosahedral order are probably similar.

Note that in figure 1(b) the temperature (8.1 K) of the first liquid configuration is slightly lower than that (8.5 K) of the last solid configuration. This is a consequence of our simulations being done in a microcanonical ensemble and not in a canonical one.

To get a better idea of what really happens to the structure as the temperature is increased, we report in figure 2 the 2D projection of the network of disclination lines connecting 'hexagonal' faces (these are the only lines present at low temperature) at three representative temperatures for the two structures (figures 2(a)–2(c): β-W; figures 2(d)–2(f): $MgCu_2$). In figures 2(a) and 2(d) we show a snapshot of the network at the temperature for which the first defect appears. These defects look very similar even though the two structures are quite different, and we will discuss this point in the following section. In figures 2(b) and 2(e) we show the disclination lines just before the melting transition, while in figures 2(c) and 2(f) the lines are shown just after the transition. It is striking that in the solid phase, even though the disorder is quite important, the underlying periodic network of disclination lines is still present and visible, while in the liquid phase it has completely disappeared.

3.2. Discussion

The first defects observed in the two cases (figures 2(a) and 2(d)) are of the same kind, and can be discussed as follows.

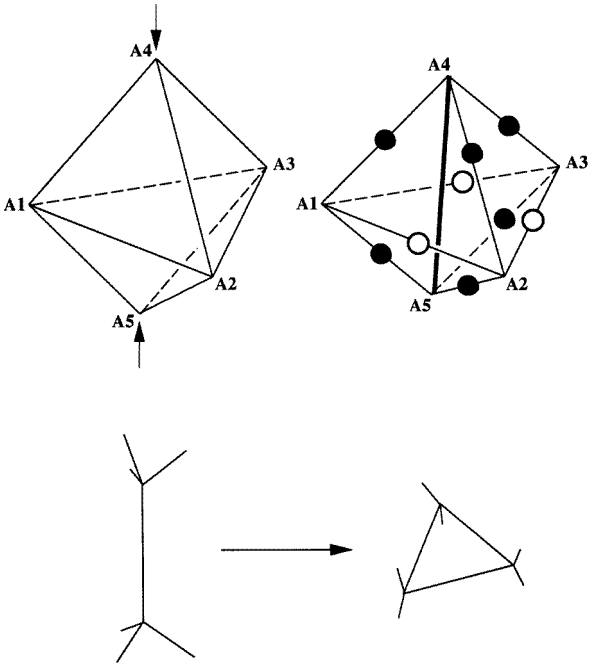

Figure 3. The initial defect mechanism (schematic): ●: +1 edge; ○: −1 edge.

Let us consider two simplicial tetrahedra ($A_1A_2A_3A_4$ and $A_1A_2A_3A_5$; see figure 3) sharing a common triangular face ($A_1A_2A_3$). If the distance (A_4A_5) between the non-common atoms becomes sufficiently small (so that one enters the circumspherical sphere

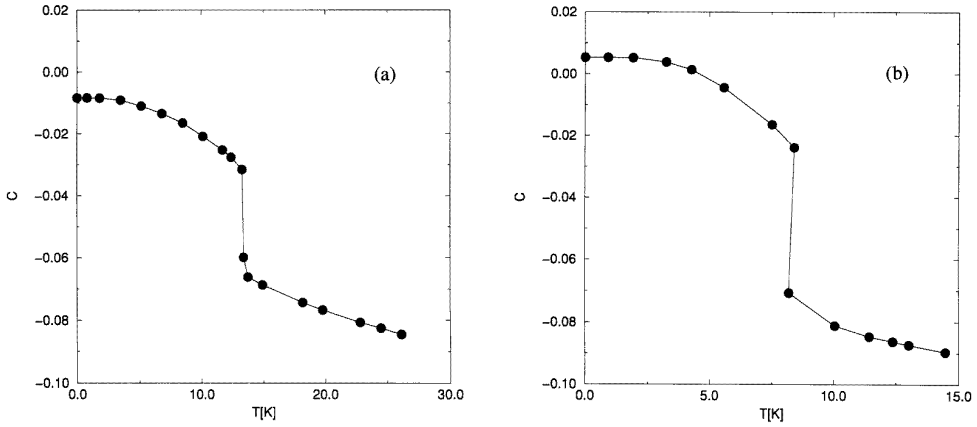

Figure 4. The quantity $c = \sum_e f_e \delta_e$ decreases with temperature, but remains close to zero. This evolution follows the decrease of the icosahedral order, with a jump at the melting temperature. The behaviour is similar for the two structures (Frank–Kasper (a) and Friauf–Laves (b)), except that positive values occur at low temperatures for the Friauf–Laves structure, related to the high connectivity of the disclination network.

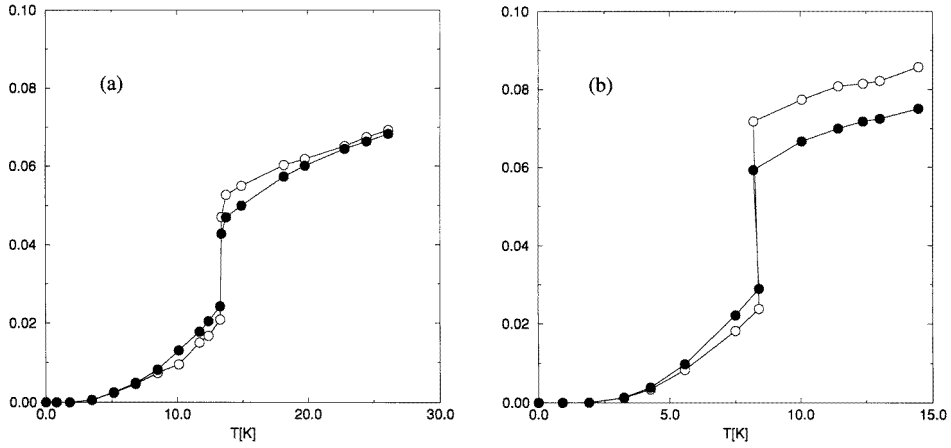

Figure 5. The evolution of f_3 (●) and $(z - z_0)/z$ (○) as functions of the temperature: (a) β-W ($z_0 = 13.5$); (b) $MgCu_2$ ($z_0 = 13.33$).

of the other tetrahedron), they become nearest neighbours, and a new Voronoï cell face is created. The two initial simplicial tetrahedra are replaced by three new tetrahedra sharing a common edge ($A_1A_2A_4A_5$, $A_2A_3A_4A_5$, and $A_3A_1A_4A_5$). Subsequently the new face becomes a triangle formed by the centres of the spheres circumscribed to these tetrahedra. The change in the topology of the Voronoï cells is summarized at the bottom of figure 3, where only the edges of the cells are sketched. As a consequence, the three faces associated with the bonds A_1A_2, A_2A_3, and A_3A_1 lose one edge, while the six faces associated with the bonds A_4A_1, A_4A_2, A_4A_3, A_5A_1, A_5A_2, and A_5A_3 gain one edge. In the A15 case, we observe that the two initial simplicial tetrahedra corresponding to the first defect to appear are such that A_4 and A_5 are at the centre and on a vertex of the cubic unit cell. This is not surprising since the distance A_4A_5 is the lowest distance not present in the

simplicial cell edges at zero temperature. Consequently, all of the faces concerned in the first defect are pentagons, so, together with the new triangle, three squares and six hexagons are created, while nine pentagons disappear. In the cubic Friauf–Laves case, we observe that the two initial simplicial tetrahedra are such that two of the three sites A_2, A_3, and A_4—for example A_2 and A_3—are Z_{16} sites, while A_1, A_4, and A_5 are Z_{12} sites. Consequently, one face (bisecting A_2A_3) is a hexagon, while all of the others are pentagons; therefore, globally, in addition to the triangle, two squares and five hexagons are created while seven pentagons disappear. In figures 2(a) and 2(d) one sees the 2D projection of the new sixfold bonds (indicated with black dots in figure 3) together with the original array of disclination lines.

In figure 4 we have monitored the quantity $c = \sum_e f_e\delta_e$. Note that, using the relation $\langle e\rangle = (6z - 12)/z$ [15], it is related to the mean coordination number z by $c = 2\pi - \alpha_t(6z - 12)/z$. As indicated above, this quantity is not a topological invariant, but remains close to zero. Its departure from zero is a measure of the disorder: it has been shown [14, 16] that a high connectivity of the disclination network increases c, while asymmetry of the Voronoï cells, or positive disclinations, decrease c. The increase of the thermal disorder caused by heating, as well as the passage from solid to liquid, contribute to lowering the value of c.

It is interesting to note that, since all of the faces were initially only pentagons and hexagons, all of the defects can be detected by counting the number of triangular faces present in the system, at least if the temperature is kept sufficiently low that these defects do not start to interact. Since one new bond is created per defect, the increase of z, $\Delta z = z - z_0$, should be equal to the number of triangular faces per atom, which is zf_3; that is

$$\frac{z - z_0}{z} = f_3. \tag{2}$$

In figure 5 we show that this relation is fulfilled at low temperature as long as the defects do not interact. Note that the creation (annihilation) process of these defects is a quite natural extension of the so-called T1 transformation previously introduced in two dimensions (here there is no analogy of the T2 transformation, as there is a natural conservation of the number of cells) [17]. This has shed new light on the importance of small triangular faces as a measure of disorder in three-dimensional structures.

Finally, close to the melting temperature, not only do these defects interact, but certainly other kinds of defect start to exist. It is interesting to consider what happens upon cooling. If the melt is cooled, as usual with this potential a glassy structure is obtained, but if the structure just below the melting temperature is cooled, the perfect structure is recovered. A few traces of the initial disclination network are sufficient for rebuilding the structure.

4. Conclusions

We have presented and discussed the results of a detailed molecular dynamics investigation of the evolution of the local structure as a function of temperature for two Frank–Kasper model systems. With use of the Voronoï tessellation we have shown that for the two systems—the β-tungsten and the $MgCu_2$ structure—the initial defects induced by raising the temperature are similar, and that the change is comparable to a T1 transformation. Moreover the results show that the disclination line network survives in the solid phase up to the solid–liquid transition temperature.

This study combines for the first time the dynamics and geometrical analysis, and gives more insight into the evolution of the local structure from the crystal to the liquid phase. The

understanding of glasses, in terms of the dynamics and the geometry, is a natural extension of this work.

Acknowledgments

We thank R Mosseri for interesting discussions concerning this work. Some of the numerical calculations were done at CNUSC (Centre National Universitaire Sud de Calcul), Montpellier.

References

[1] Frank F C and Kasper J S 1958 *Acta Crystallogr.* **11** 184
Frank F C and Kasper J S 1959 *Acta Crystallogr.* **12** 483
[2] Janot C 1992 *Quasicrystals: a Primer* (Oxford: Oxford University Press)
Hippert F and Gratias D (ed) 1994 *Lectures on Quasicrystals* (Paris: Editions de Physiques)
[3] Schoemaker C B and Schoemaker D P 1989 *Aperiodicity and Order 3: Extended Icosahedral Structures* ed M Jaric and D Gratias (New York: Academic)
[4] Sadoc J F 1983 *J. Physique Lett.* **44** 707
Nelson D R 1983 *Phys. Rev. Lett.* **13** 983
[5] Laird B and Schober H 1991 *Phys. Rev. Lett.* **66** 636
[6] Bembenek S D and Laird B B 1995 *Phys. Rev. Lett.* **74** 936
Schober H R and Oligschleger C 1996 *Phys. Rev.* B **53** 1
Caprion D, Jund P and Jullien R 1996 *Phys. Rev. Lett.* **77** 675
[7] Steinhardt P J, Nelson D R and Ronchetti M 1983 *Phys. Rev.* B **28** 784
[8] Bernal J 1964 *Proc. R. Soc.* A **280** 299
[9] Finney J 1993 *Disorder and Granular Media* ed D Bideau and A Hansen (Amsterdam: North-Holland–Elsevier) p 35
[10] Hoare M R 1978 *J. Non-Cryst. Solids* **31** 157
[11] Jullien R, Jund P, Caprion D and Quitmann D 1996 *Phys. Rev.* E **54** 6035
[12] Rivier N and Sadoc J F 1988 *Europhys. Lett.* **7** 526
[13] Sadoc J F and Mosseri R 1989 *Aperiodicity and Order 3: Extended Icosahedral Structures* ed M Jaric and D Gratias (New York: Academic) p 163
Mosseri R and Sadoc J F 1995 *Geometry in Condensed Matter Physics (Directions in Condensed Matter Physics 9)* ed J F Sadoc (Singapore: World Scientific) p 239
[14] Sadoc J F and Mosseri R 1984 *J. Physique* **45** 1025
[15] Rivier N 1993 *Disorder and Granular Media* ed D Bideau and A Hansen (Amsterdam: North-Holland–Elsevier) p 55
[16] Rivier N 1982 *J. Physique Coll.* **43** C9 91
[17] Weaire D and Rivier N 1984 *Contemp. Phys.* **25** 59